COMBUSTION CONTROL AND DIAGNOSTICS SENSOR TESTING IN A THERMAL BARRIER COATED COMBUSTOR

B. T. Chorpening, M. G. Dukes*, P. Pich*, and J. D. Thornton
National Energy Technology Laboratory
Morgantown, WV 26507, USA

ABSTRACT

The combustion control and diagnostics sensor (CCADS) continues to be developed as an in-situ combustion sensor, with immediate application to natural gas fired turbines. In-situ combustion monitoring is also expected to benefit advanced power plants of the future, fueled by coal-derived syngas, liquified natural gas (LNG), hydrogen, or hydrogen blend fuels. The in-situ monitoring that CCADS provides can enable the optimal operation of advanced, fuel-flexible turbines for minimal pollutant emissions and maximum efficiency over the full operating range of an advanced turbine. Previous work has demonstrated CCADS as a useful sensor for in-situ monitoring of natural gas combustion, including detection of important combustion events such as flashback and lean blowoff, in experimental combustors without thermal barrier coatings (TBC). Since typical TBC materials are electrical insulators at room temperature, and CCADS operation requires conduction of electrical current to the walls of the combustor, a TBC on the combustion liner was identified as a potential barrier to CCADS operation in commercial application. This paper reports on CCADS experiments in a turbulent lean premixed combustor with a yttria-stabilized zirconia (YSZ) thermal barrier coating on the combustor wall. The tests were conducted at 0.1 MPa (1 atm), with a 15V excitation voltage on the CCADS electrodes. The results confirm that for a typical thermal barrier coating, CCADS operates properly, and the total measured average resistance is close to that of an uncoated combustor. This result is consistent with previous materials studies that found the electrical resistance of typical TBC materials considerably decreases at combustor operating temperatures.

INTRODUCTION

The United States Department of Energy (DOE) National Energy Technology Laboratory (NETL) conducts programs that support the global interest for clean power generation such as the Turbine Program. DOE programs are also concerned with future power generation problems associated with issues such as increased imports of liquefied natural gas (LNG), which may affect the pipeline fuel properties enough to impact the performance of modern power turbines. Many performance and operational concerns can be mitigated by integrating combustion sensors and controls to facilitate fuel-flexible fine tuned control over a larger range of operating conditions. Advanced power plants of the future, which are likely to be fueled with coal-derived syngas, hydrogen, and hydrogen blends, will also benefit from the integration of combustion sensors and controls to maintain high performance while avoiding combustion instabilities, particularly flashback. In support of the goals of the Turbine Program, researchers at NETL are developing sensor technology for combustion monitoring and control. This sensor development is based on using the flame's electrical properties to perform real-time diagnostics and in-situ monitoring of critical combustion

* Mickey Leland Energy Fellowship student

This material is declared a work of the U.S. Government and is not subject to copyright protection in the United States. Approved for public release; distribution is unlimited.

parameters, including flashback, lean blowout, combustion dynamics, and equivalence ratio [1-6].

It is well known that a flame can conduct electrical current [3],[9],[10],[11] and that the measured current conducted through the flame relates to the flame characteristics. The flame ionization detector (FID) used in gas chromatography [9],[10] uses the measured current through a small, well-controlled flame to measure very low concentrations of hydrocarbons. The reaction most often cited for providing the FID response results from the chemi-ionization of CHO* [9],[10]:

$$CH + O \rightarrow CHO^* \rightarrow CHO^+ + e^- \qquad (1)$$

In a FID, use of a small, well-controlled flame, and application of sufficient voltage allows complete collection of the generated electrons. The number of electrons produced has been found to be proportional to the number of hydrocarbons in the sample, with modifications for specific functional groups such as –OH. An extensive review of past research in flame ionization has been published by Fialkov [12].

In most practical combustion systems, mass flow rates are orders of magnitude higher than the flow rates in a FID. This makes complete charge collection very difficult (i.e., requiring very high electric field strength). However, a representative signal at various conditions may be obtained at relatively low electric field strengths.

Modern gas turbines are manufactured with thermal barrier coatings on the combustor liner and hottest turbine blades and vanes to reduce metal temperatures and provide corrosion protection [8]. TBCs protect the metal substrate from elevated temperatures by sustaining a high thermal gradient if adequate backside cooling of the metal is present. As a result the service life of a gas turbine combustor liner or airfoil is prolonged. Further benefits include cost reduction as less exotic materials can be used for the component design and the increase of fuel efficiency by operating at higher temperatures with reduced cooling flows. Typically, these coatings have an insulating layer are 100-300 um thick, and are based on ZrO_2-Y_2O_3 (YSZ). At room temperature, these materials are good electrical insulators. In preliminary tesing, discussed in detail later, the resistivity of a ZrO_2-8%Y_2O_3 coating was measured to be $2*10^9$ ohm-cm at room temperature. In comparison, the resistivity of NiCr (80/20) is about $1*10^{-4}$ ohm-cm [13], and the resistivity of alumina (Al_2O_3) is about $1*10^{14}$ ohm-cm. To operate, CCADS needs to be able to conduct electrical current through the flame to the walls of the premixer and combustor, so the presence of an electrically insulating coating on the combustor wall is a concern.

Variations of YSZ are used as solid electrolyte in solid oxide fuel cells. Studies have shown that the conductivity of pressed and sintered YSZ improves significantly with increased temperature [14],[15]. Prior to the tests reported within, experimental combustors used in the development and testing of CCADS at NETL did not have thermal barrier coatings. To confirm that a thermal barrier coating would not prevent CCADS from operating properly, tests were performed in an atmospheric pressure combustor with a common YSZ TBC.

NOMENCLATURE

FID	flame ionization detector
TBC	thermal barrier coating
Pf	premixer fuel plenum pressure
Pn1	premixer nozzle pressure near combustor
Pn2	premixer nozzle pressure upstream of Pn1
PSD	power spectral density
Vref	reference velocity (average inlet velocity)
YSZ	yttria stabilized zirconia
Φ	equivalence ratio

PRELIMINARY COUPON TESTING

Hastelloy X coupons with dimensions 2.875 x 2.875 x 0.635 cm (1.125 x 1.125 x 0.25 in.) were coated by a commercial TBC vendor with three different TBCs (products of Praxair and Sulzer-Metco), described in Table 1. Hastelloy X is an austenitic high chrome-nickel alloy used in applications that require high temperature conditions, with a melting range between 1260-1355°C. One set of the samples were coated only with the bond coat.

TBC type	Thickness	Chemistry
Metco 204 NS	15 mils	ZrO_2 8%Y_2O_3
Metco 204 NS	30 mils	ZrO_2 8%Y_2O_3
Metco 202 NS	15 mils	ZrO_2 20%Y_2O_3
ZRO-103	15 mils	ZrO_2 22%MgO
Bond Coat	5-6 mils	51%Ni-22%Co-21%Cr-5%Al-1%Y

Table 1. Chemistry and thickness of various TBC components.

A nichrome wire was spot welded to the uncoated side of each sample, to provide one of the lead wires necessary for the impedance measurements of the TBC material. To attach a secondary lead wire to the TBC, a 1 cm^2 platinum pad was sputtered onto the thermal barrier coating. A MED 010 Blazers Union sputtering device was employed. In order to achieve a uniform thickness for the electrode contact on a porous TBC a 0.5 micron coating of platinum was applied. Each sputtered pad was then placed in contact with a platinum mesh with a platinum wire (26 gage ~ 0.015 in. diameter) attached to it. SPI platinum paint was applied to attach the electrode and the entire assembly was sintered in a Lindberg electric furnace at 500°C for a few minutes.

Room temperature direct current (DC) resistance readings were performed using a Fluke 189 digital multimeter. Initial resistance measurements across the Hastelloy X coupon (no

TBC) showed very small resistances at various points. The average measured resistance was 0.3 Ω. The 50 in. platinum wire showed a resistance of 1.3 Ω, while the 25 in. nichrome wire had a resistance of about 1.2 Ω. For a specimen with a TBC the resistance across the TBC was outside of the range of the voltmeter, or in excess of 100 MΩ. This resistance at room temperature is high enough to cause difficulty with the operation of the CCADS electronics.

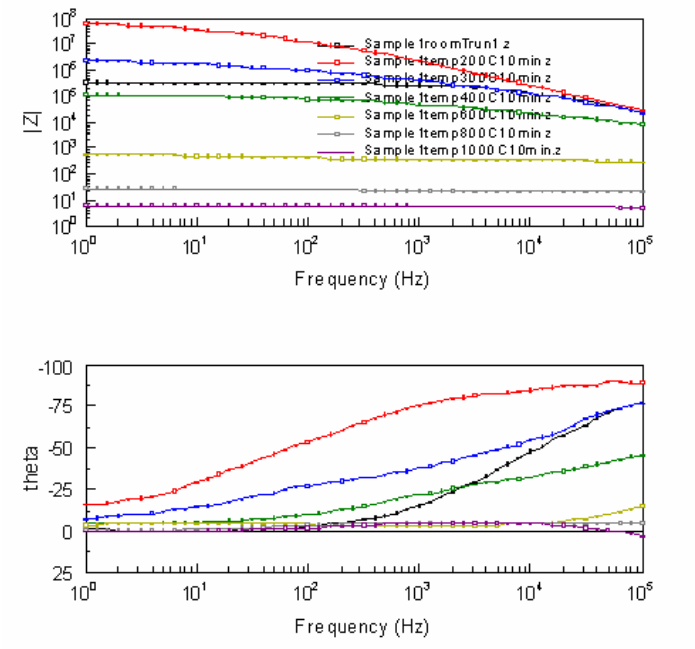

Figure 1. Impedance measurements of sample coupon with Sulzer-Metco 204 NS coating, at temperatures up to 1000°C.

Impedance testing was performed using a Solartron SI 1287 Electrochemical interface and a SI 1260 Impedance/Gain-Phase Analyzer. Spectra analyses were done using Zview impedance analysis software (Scribner Associates, Inc.). In the measurements, an alternating current amplitude of 3V was employed over a frequency range from 1 Hz to 100 kHz. The samples were placed inside a Lindberg electric furnace on a refractory cylinder. Each sintered platinum electrode was wedged in between a refractory material and mica to ensure that it did not separate from the sample. The impedance testing was conducted on the samples at various temperatures up to 1000°C.

Results for the 380 μm (15 mil) thick Sulzer Metco 204NS thermal barrier coating are shown in Figure 1. It had high impedance values at room temperature (about 2 GΩ at low frequency). From the area and material thickness, the resistivity is calculated. As the temperature was increased in the range of 200°C, the impedance values increased. Above 200°C, the impedance decreased. As the temperature reached 1000°C, the sample impedance dropped to values below 100 Ω. This means that the conductivity of these ceramic materials went up with increasing temperature. This increased conductivity is most likely ionic in nature, as such a behavior of yttria stabilized zirconia electrolyte material (for fuel cells) has been reported previously [15]. The samples with only a bond coat had low impedance at all temperatures. The remaining TBC materials behaved in a manner similar to the Metco 204NS, with high impedance at room temperature, but falling to below 100 Ω by 1000ºC.

ATMOSPHERIC COMBUSTOR TESTING

The testing was performed in the Low Pressure Demonstration Combustor facility using a new generic combustor with a thermal barrier coating. The combustor is shown in Figure 2. The combustion chamber has an internal length of 610 mm (24 in.).

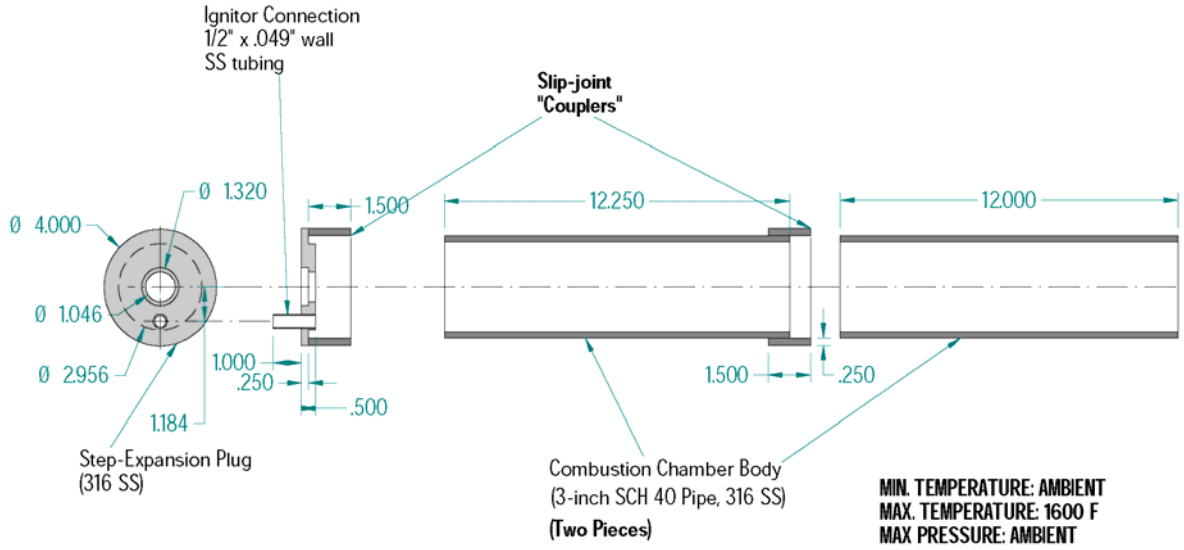

Figure 2. Atmospheric pressure combustor used in experiments (dimensions in inches).

Figure 3. View from the combustor exhaust, showing the white thermal barrier coating on the combustor wall. Pilot flame inlet is to the right of the premixer inlet.

The coated combustor is mounted inside a stainless steel, atmospheric pressure chamber to contain the process gases and protect laboratory personnel. Excess air flows through the protective chamber around the outside of the combustor, and mixes with the combustion products to cool the combustor and exhaust. The premixer is attached to the center of the inlet end of the combustor. A second inlet for the pilot flame is also in the inlet wall of the combustor. The pilot was only used until the main fuel/air mix was ignited and stabilized.The combustor was constructed in three pieces to allow for application of the thermal barrier coating. The coating was applied by a professional TBC company using a plasma spray process. The bond coat, Praxair NI-171 was applied to a thickness of 125-200 µm (0.005 – 0.008 in.), and followed with a top coat of Metco-204 (ZrO_2 - 8% Y_2O_3) to a thickness of 250-380 µm (0.010 – 0.015 in.). The resulting coating covers the entire inside wall of the combustor, as shown in Figure 3.

Figure 4 shows the construction of the lean premix fuel nozzle which is at the head of the combustor. Two pressure transducers, Pn1 and Pn2, are mounted on the premixer. The transducer closest to the combustor, labeled Pn1, has been used for monitoring combustion dynamics. The Pf pressure transducer monitors the pressure in the fuel plenum. The two CCADS electrodes are incorporated into the construction of the centerbody. The inside diameter of the premixer is 26.6 mm (1.05 in.). A swirler is located at the premixer entrance shortly before fuel injection. The tip of the premixer centerbody is flared to provide local flow acceleration, which encourages the flame to anchor downstream of the premixer exit. The guard electrode covers the last 9.8 mm (0.39 in.) of the premix injector centerbody at the combustor inlet. The sense electrode covers the next 4.1 mm (0.16 in.) of the centerbody upstream of the guard electrode. Both are electrically isolated from the rest of the centerbody. The guard electrode is nearest the combustion zone. The sense electrode is just upstream of the guard electrode. The arrangement of the electrodes facilitates current flow from the guard electrode through the flame in the combustion zone to the combustor wall. Due to the locally symmetric electric field imposed by the combination of the guard and sense electrodes, a significant ionization current from the sense electrode is produced only when the flame enters the premixing region of the fuel injector (i.e., auto-ignition, and flashback). A constant bias of +15V is applied to all electrodes. The current flow from each electrode is read independently through a prototype system built at NETL. Data is recorded at 12 kHz on a TEAC data recorder.

An acoustic resonator is attached to the fuel plenum which encircles the premixer. This variable quarter wave resonator allows the operator to tune the acoustics of the fuel injection system. This is discussed by Richards et al [16]. In these tests,

the acoustic tuner is used to change the magnitude and frequency of the combustion oscillations.

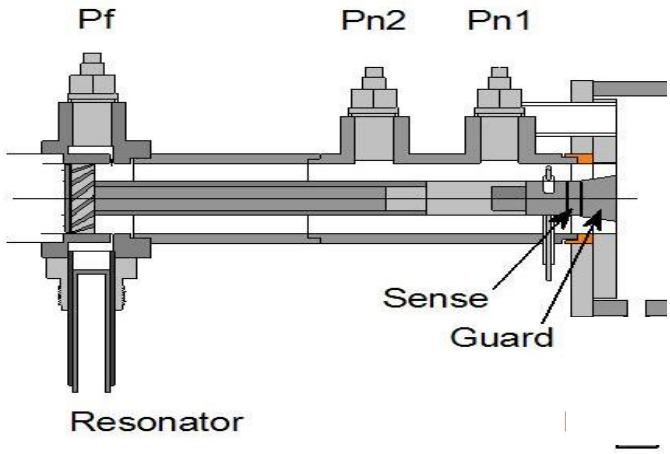

Figure 4. Detail of premix injector nozzle.

Tests were run with reference velocities from 20 m/s to 30 m/s, at equivalence ratios of 0.6 and 0.7. This paper will focus on the data obtained with a reference velocity of 20 m/s.

DATA ANALYSIS

The Guard and Sense current and the three pressure transducers signals are recorded at 12 kHz. For the Guard and Sense electrodes, voltage signals are produced by the electronics representing the current. The voltage signal is converted to current using the calibration curve for the CCADS electronics shown in Figure 5. The power spectral density is calculated using data blocks of 4096 points, with a Hanning window, and averaging over approximately 10 seconds of data.

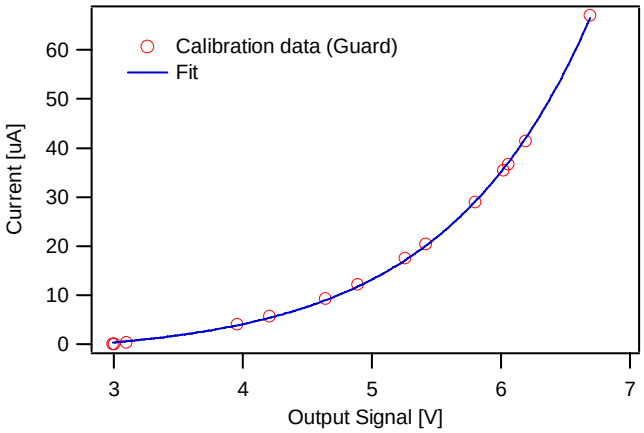

Figure 5. Calibration curve for flashback electronics with current limiting resistor.

RESULTS

An example of the data is shown in Figure 6, a condition with Vref = 20 m/s, and Φ = 0.7. The sense electrode signal shows the flame is occasionally flickering back into the premixer at this condition, but that the flame is not anchored in the premixer. The guard electrode has a stronger signal, showing an average current near 3.4 μA, with oscillations in phase with the combustion pressure oscillations (Pn1). The fuel plenum (Pf) pressure signal also shows higher frequency content which does not appear to carry downstream to the outlet of the nozzle.

For comparison, Figure 7 shows data from a previous experiment performed in a somewhat similar combustor without a TBC coating [6]. The same premix injector design was used, and the combustor diameter was the same as the present work. A pressure transducer port was connected directly to the combustor wall. The combustor tube, 927 mm (36.5 in.) long, was considerably longer than the TBC coated combustor used in the present experiments. As a result, the dominant frequencies of the uncoated combustor are considerably lower. As in Figure 6, the operating condition was Vref = 20 m/s, Φ = 0.7.

Despite the differences between the uncoated and coated combustors, it is apparent that the general behavior of the guard electrode signal is similar between the two. For the condition shown in Figure 6, the average guard electrode current was 1.26 μA, with an applied voltage of 5V. This results in an average resistance of 4.0 Mohm with the uncoated combustor. In comparison, the TBC coated combustor data shown in Fig 5 has an average guard electrode current of 3.35 μA with an applied voltage of 15V. This results in an average resistance of 4.5 Mohm. Thus, the TBC coating has not produced a large change to the electrical resistance of the system in operation. This small change is likely due to small changes in the flame structure caused by shorter combustor length and the higher combustion gas temperature achieved with the TBC coating.

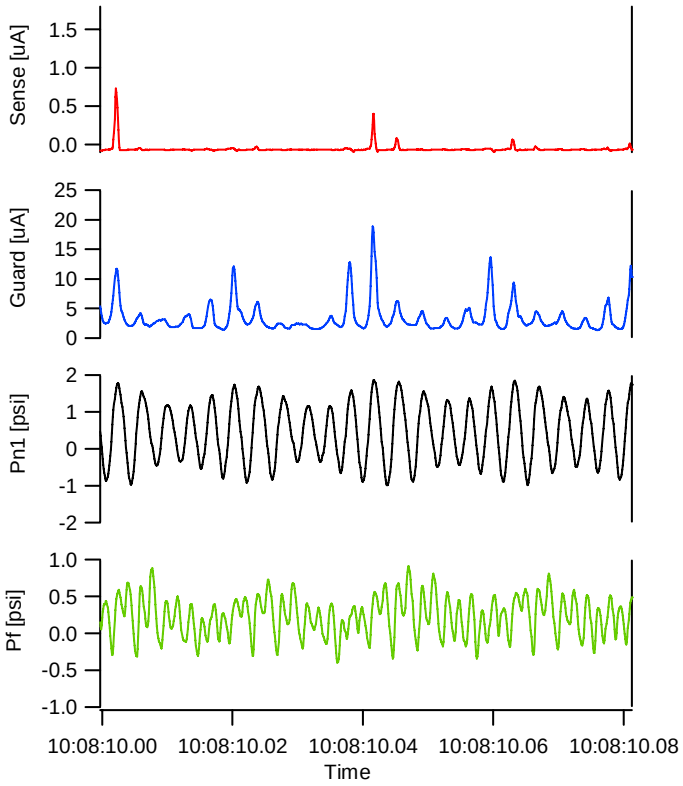

Figure 6. Example of real time data from TBC coated combustor, with Vref = 20 m/s, and Φ = 0.7.

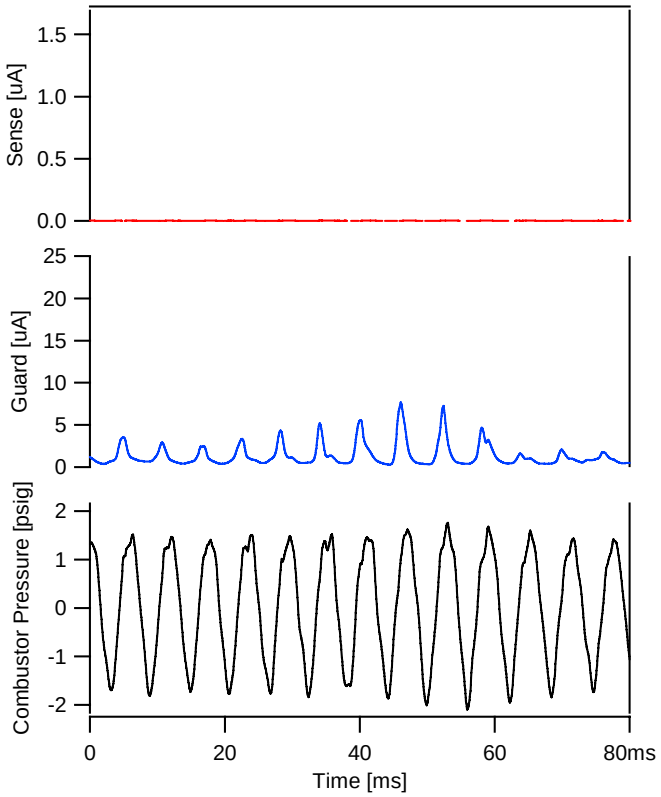

Figure 7. Real time data from uncoated combustor with Vref = 20 m/s, and Φ = 0.7.

The power spectral density for each data set is computed using IGOR Pro v.5. Figure 8 shows the PSD for 10 seconds of data at the condition shown in Figure 6. The dominant frequency, 278 Hz, appears distinctly in both Guard and Pn1 signals.

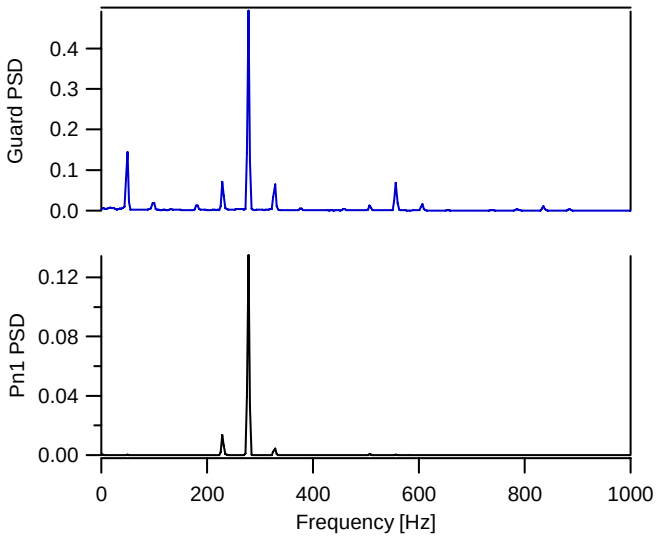

Figure 8. Power spectral density of example data from TBC coated combustor in Figure 6.

For this discussion, the dominant frequency is defined as the frequency with the *highest* PSD amplitude. Figure 9 shows the PSD amplitude at the dominant frequency of 14 data sets, for both the nozzle pressure transducer and the Guard current. All 14 data sets have an equivalence ratio of 0.7 and a reference velocity of 20 m/s. For every data set the length of the resonator attached to the fuel manifold is changed, which affects the fuel system acoustics, and in turn the combustion dynamics. The frequency correspondence between the dominant peaks in the guard and Pn1 signals is very good, with a difference at a resonator length of 685 mm, at a condition with weak pressure oscillations near a stability boundary. The amplitude of both the guard and Pn1 behave similarly as the resonator is adjusted.

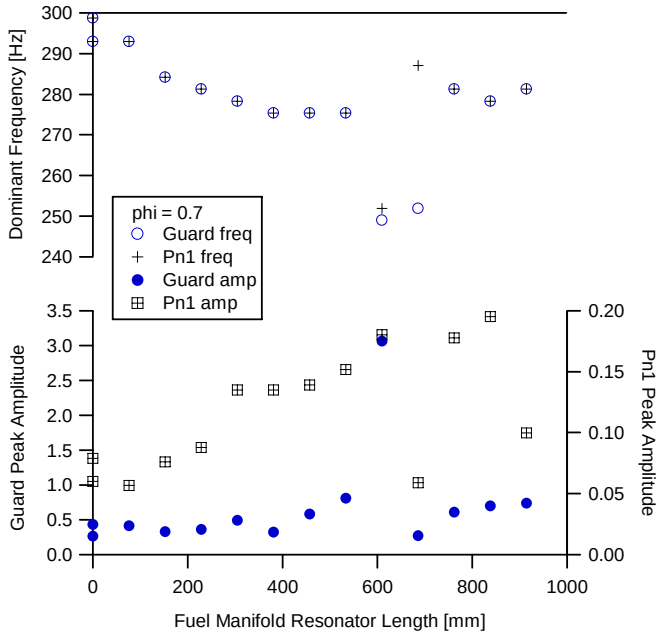

Figure 9. Comparison of Guard and Pn1 PSD peaks at Φ = 0.7 and Vref = 20 m/s.

Figure 10 shows the PSD amplitude at the dominant frequency for 14 data sets with an equivalence ratio of 0.6 and a reference velocity of 20 m/s. For every data set the length of the resonator attached to the fuel manifold is changed, which affects the fuel system acoustics, and in turn the combustion dynamics. The frequency correspondence between the dominant peaks in the guard and Pn1 signals is not as good as at Φ = 0.7. The four points which do not match in frequency are those with the weakest pressure oscillations in the data set.

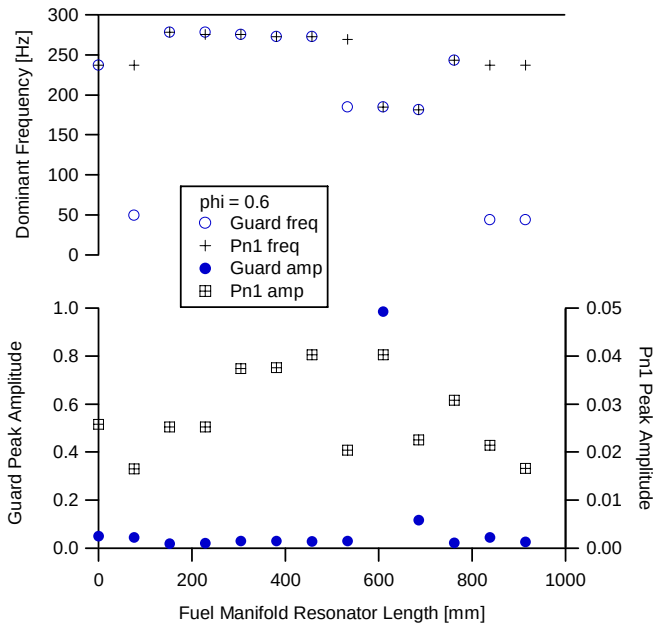

Figure 10. Comparison of Guard and Pn1 PSD peaks at Φ = 0.6.

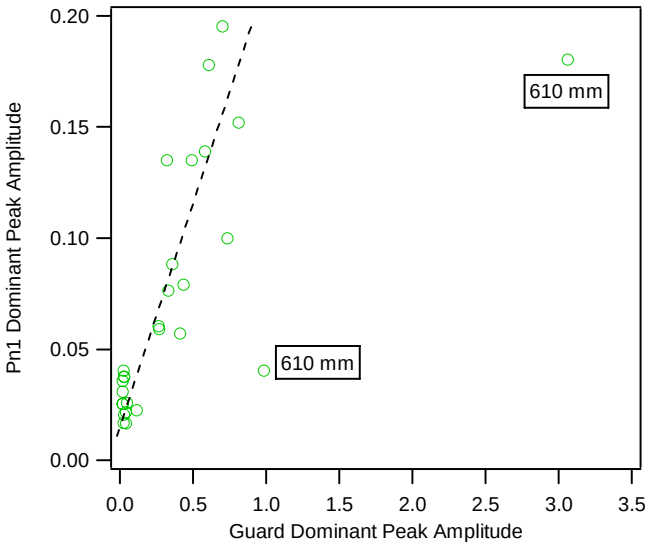

Figure 11. Guard ion signal and nozzle pressure amplitudes.

The data in Figure 11 show that most of the data demonstrate that the amplitude of the dominant pressure peak is correlated with the amplitude of the dominant guard oscillation peak. The two outliers occur when the resonator length is 610 mm, which is a peak near a mode shift or stability boundary. During operation, when moving to those points the primary frequency shifts suddenly from about 275 Hz to 252 (Φ = 0.7), or from 272 to 185 Hz (Φ = 0.6).

CONCLUSIONS

Modern turbine systems employ thermal barrier coatings to increase the life of critical hot section components. At room temperature, common thermal barrier coating materials, such as YSZ, are electrical insulators. Although preliminary coupon tests showed common TBC materials to decrease in resistance at elevated temperatures, the operation of the Combustion Control and Diagnostic Sensor (CCADS) in a combustor with a TBC had not been previously demonstrated at NETL. This testing demonstrated CCADS detection of flame flickering back into the premixer, and monitoring the amplitude and frequency of combustion dynamics as part of a multi-function sensor installed in a generic combustor with a TBC. Average flame resistance values were similar to those obtained from testing in an uncoated combustor, indicating the TBC coating did not add considerable resistance to the system in operation. This reduces the barrier to implementation in gas turbines in service, since combustor liners with thermal barrier coatings will still allow the sensor to function properly. This leaves modification of commercial fuel injector designs to incorporate CCADS electrodes as the main engineering barrier to implementation.

Future work on CCADS at NETL will focus on improving algorithms for measuring equivalence ratio, including in systems with fuel variability. The recent addition of a propane fuel system at NETL allows for the blending of natural gas and propane in the fuel supply to high pressure combustors, to examine mixtures representative of LNG. The high pressure combustion facility also has hydrogen available for testing CCADS performance with pure hydrogen and high-hydrogen blends.

ACKNOWLEDGMENTS

The authors wish to thank Mr. Ed Robey and Mr. Rick Addis (Research and Development Solutions – Parsons Inc.) for their support of the setup and operation of the experiments, and Mr. Bill Fincham (Research and Development Solutions – Parsons Inc) for his electronics support.

REFERENCES

[1] Thornton, J., Richards, G.A., and Robey, E., "Detecting Flashback in Premix Combustion Systems." Presented at the American Flame Research Committee International Symposium, Newport Beach, California, 2000.

[2] US Patent 6,429,020. J. D. Thornton, G. A. Richards, D. L. Straub, E. A. Liese, J. L. Trader, G. E. Fasching, *Flashback detection sensor for lean premix fuel nozzles,* 2002.

[3] Benson, K., Thornton, J. D., Straub, D. L., Huckaby, E. D., Richards, G. A., "Flame ionization sensor integrated into gas turbine fuel nozzle," GT2003-38470, Proceedings of Turbo Expo 2003, June 16-19, Atlanta, GA.

[4] Thornton,J., Straub, D., Chorpening, B., Huckaby, E.D., Richards, G.A., and Benson, K., "A Combustion Control And Diagnostics Sensor For Gas Turbines," ASME Paper GT2004-53392.

[5] Chorpening, B. T., Straub, D. L., Huckaby, E. D., Benson, K. J., "Detection of lean blowout and combustion dynamics using flame ionization," ASME Paper GT2005-68612, Proceedings of Turbo Expo 2005, Reno, NV, June 6-9.

[6] Chorpening, B. T., Huckaby, E. D., Morris, M. L., Thornton, J. D., Benson, K. J., "Flame Ionization Distribution and Dynamics Monitoring in a Turbulent Premixed Combustor." GT2006-90879, Proceedings of Turbo Expo 2006, May 8-11, Barcelona, Spain.

[7] Thornton, J. D., Chorpening, B. T., T. G. Sidwell, P. A. Strakey, E. D. Huckaby, K. J. Benson, "Flashback Detection Sensor for Hydrogen Augmented Natural Gas Combustion," ASME Paper GT2007-27865, Proceedings of Turbo Expo 2007, May 14-17, Montreal, Canada.

[8] Boyce, M. P., *Gas Turbine Engineering Handbook, 2nd Ed.*, 2002, Butterworth-Heinemann, pp. 433.

[9] Cheng, W.K., Summers, T., and Collings, N., "The Fast-Response Flame Ionization Detector." *Prog. Energy Combust. Sci.*, v24, 1998, pp. 89-124.

[10] Holm, T., "Aspects of the Mechanism of the Flame Ionization Detector." *Journal of Chromatography A*, v842, 1999, pp. 221-227.

[11] Calcote, H. F., "Electrical properties of flames: burner flames in transverse electric fields," *The Third Symposium on Combustion, Flame, and Explosion Phenomena*, pp. 245-253, 1949.

[12] Fialkov, A.B., "Investigations on Ions in Flames." Prog. Energy Combust. Sci., v23, 1997, pp. 399-528

[13] Fink, D. G., and Beaty, H. W., Eds., *Standard Handbook for Electrical Engineers*, 12th Ed, 1987, p.4-75.

[14] Kurumada, M., Hara, H., and Iguchi, E. "Oxygen vacancies contributing to intragranular electrical conduction of yttria-stabilized zirconia (YSZ) ceramics," *Acta Materialia*, 2005, v. 53, pp.4839-4846.

[15] Chen, X.J., Khor, K.A., Chan, S.H., and Yu, L.G. "Influence of microstructure on the ionic conductivity of yttria-stabilized zirconia electrolyte," *Materials Science and Engineering*, A335 (2002), pp. 246-252.

[16] Richards, G., Straub, D., and Robey, E., "Control of combustion dynamics using fuel system impedance," GT2003-38521, Proceedings of Turbo Expo 2003, June 16-19, Atlanta, GA.